Novel composite polybenzimidazole-based proton exchange membranes as efficient and sustainable separators for microbial fuel cells

S. Angioni, L. Millia, G. Bruni, D. Ravelli, P. Mustarelli[*] and E. Quartarone

Department of Chemistry, University of Pavia and INSTM, Via Taramelli 12, 27100, I-Pavia, Italy

*piercarlo.mustarelli@unipv.it

Abstract

Microbial fuel cells (MFCs) are gaining increasing technological relevance for wastewater remediation and ancillary energy production. MFC separators are often fabricated with ion-exchange perfluorinated membranes, the most common of them being Nafion[TM]. Here, we prepared composite separators based on polybenzimidazole (PBI), where the filler is made of SBA-15 mesostructured silica functionalized with sulphonic moieties. These membranes allowed strong increase of power density (up to one order of magnitude), operating life and wastewater treatment efficiency with respect to Nafion[TM]. Moreover, our sustainability and cost analysis clearly showed that PBI is more convenient than Nafion[TM] for making these membranes. Therefore, we conclude that PBI-based membranes are very promising as separators for MFCs.

Keywords: polybenzimidazole, microbial fuel cells, biomass, wastewater, proton exchange membranes.

1.**Introduction**

Microbial fuel cells (MFCs) are bioelectrochemical systems (BES) that produce electricity from anodic oxidation reactions catalysed by bacteria. Although the electrochemical effects caused by the activity of microorganisms have been known since the early 20th century, MFC is now considered an innovative technology, due to its possible employment in a wide spectrum of green and sustainable applications, as production of bio-hydrogen, water/soil bioremediation and environmental sensing [1,2].

A relevant potential of MFCs comes out from the possibility to combine wastewater treatment and bioenergy harvesting, namely using municipal and/or industrial wastewaters as the fuel [1, 3]. At present, the current technologies for wastewater treatment, such as the activated sludge systems based on aerobic bioreactors, are energy-consuming and require high investments. In contrast, MFCs could offer a sustainable pathway for several reasons including energetic, economic, environmental and operating factors. First, they directly recover bioelectricity and other valuable products from the degradation of the wastewater organic substrate with no need of aeration. They even allow a good effluent quality, which is an important requirement to meet water reclamation, and have low environmental footprint (mostly low-carbon), due to a successful combination of biological processes and electrochemical reactions. Finally, the MFC design may include real-time monitoring and control [2].

In terms of working efficiency, it has been reported that, in case of domestic wastewater treatment, a MFC would only consume 0.024 kW on average (mainly for reactor feeding), which is roughly one order of magnitude less than conventional aerobic processes based on activated sludge (about 0.3 kW) [2]. Unfortunately, while the MFC wastewater treatment is undoubtedly sustainable on small scales (e.g. 1 dm^3), the breakeven point is much more difficult to reach on the larger scales (~1 m^3) required by real applications. The major limiting drawback concerns the power output. Small MFCs produce a maximum power density of about 1 W m^{-3}, which is 1000 times lower than the target value of 1 kW m^{-3} typical of an organic loading rate of 10 kg-COD m^{-3} day^{-1} [see ref. 2 for further details]. Such a functional issue is a direct consequence of different device bottlenecks, e.g. low conductivity, pH-buffering action of several wastewaters, nature of microbial community etc [4].

During the last decade, better performances were achieved by optimising some cell factors, even if the matching of power produced by chemical fuel cells could not be practically expected for several reasons, the most important of which is likely the inherent slowness of bio-conversion

if compared with chemical one. Indeed, important improvements were obtained by implementing sophisticated cell architectures, as for instance dual-chamber, single-chamber, tubular, plane and stacked MFCs, but also by developing new materials for the electrodes and the separator [5-8]. In case of dual-chamber (or H-cell), the anode and the cathode are placed in two distinct compartments, separated by a membrane. On the contrary, the single-chamber fuel cell is composed by a single anode compartment, whereas the cathode is directly exposed to air. The open-to-air cathode architecture is often used in membrane-less configuration, even if a membrane may be sometimes used and in this case, it is hot-pressed onto the cathode surface to form a membrane-electrode assembly (MEA). Tubular MFC has cylindrical geometry. In this configuration, MEA is wrapped around the centrally positioned anode, whereas the cathode is exposed to the air. Finally, plane MFC are rectangular-shaped and the membrane-electrode assembly is sandwiched between two plates including the flow-channels, necessary for the wastewater flow at the anode and of the air at the cathode. Each architecture shows advantages and disadvantages. The single-chamber MFC, for instance, has a simple design, lower cost and higher efficiency, mostly in case of membraneless configuration. In contrast, it has limited application and suffers cathode biofouling and high oxygen crossover, when no membrane is present. The double-chamber fuel cell is a more versatile system, but a membrane is required to separate the compartment, avoid contamination and protect the cathode. The critical issues still concern higher production cost and lower efficiency related to the membrane resistance [5-8].

A MFC is made of an anode, where the bacteria oxidize the wastewater organic substrate, so producing electrons collected in the external circuit and protons that migrate toward the cathode through a membrane (separator). Separators strongly affect the MFC operation because of many drawbacks, including high internal resistance, biofouling, pH splitting, O_2 diffusion and substrate loss across the membrane [8, 9]. As a matter of fact, an ideal membrane for MFC should satisfy the following requirements: i) low cost; ii) low ionic resistance to facilitate the proton migration from the anode to the cathode; iii) non-porous microstructure to avoid the oxygen diffusion and substrate crossover; iv) high resistance to biofouling to preserve the cell from loss of performance.

The most common separators used in MFCs are cation exchange membranes (CEM), anion exchange membranes (AEM), composites and porous materials (both organic and inorganic), as glass fibers, J-cloths, nylon filters, non-woven cloths, ceramics [9-11]. Among them, porous systems show the lowest ohmic resistance but are also permeable to O_2, whereas the dense ones may be highly proton-conducting but not cost-effective. In addition, until now, none of the

investigated separators could avoid the biofilm growth on the membrane surface, which causes serious drops of the performances.

Proton-exchange membranes (PEMs) are frequently used as separators for MFCs and, among them, Nafion^{TM} and Nafion-like matrices are the most investigated systems. Compared to other separators, in fact, they show high proton conductivity and low internal resistance [11]. On the other hand, Nafion^{TM}-based PEMs are expensive, undergo both chemical and biological biofouling, and suffer of high transfer ratio of cations coming from the substrate, so hindering the cathode electrochemical reaction. Given these problems, the search for innovative and advanced membranes is an important scientific and technical issue.

Polybenzimidazole (PBI) is a good alternative to Nafion^{TM} in chemical fuel cells [12]. In fact, it is cheaper than Nafion^{TM}, easy to synthesize and process, and chemically stable. Recently, membranes of PBI-PVP and of sulfonated oxyPBI were investigated as separators for MFCs, by using synthetic and sludge-activated wastewaters, respectively. Promising results were also obtained in terms of power output. However, these cells must be further improved for what concerns the long-term stability [13, 14].

Here, we report on the use of novel PEMs based on poly-(2,6-pyridine-2,2-phenilenebenzimidazole) (Py-PBI) as separators in MFCs for municipal wastewater treatment. The membranes were prepared both as single-phase materials, as well as in form of composites obtained by dispersing different types of filler in the polymer, namely SBA-15 mesoporous silica and SBA-15 properly functionalized with sulphonic groups, -SO$_3$H. In order to focus the attention on the membrane properties and to better compare the separators, we adopted a simplified device geometry, that of a single-chamber open-air MFC (see Scheme in the Experimental Section). Long-term electrochemical experiments were carried out to investigate the MFC functional stability, which was compared to that of Nafion^{TM}-based cells. A sustainability assessment of the proposed systems is also reported, which considers both cost- and environment-effectiveness of the chosen materials.

1.Experimental Section

2.1   MFC Assembly

2.1.a Preparation of the PBI-based membranes

4

Poly-2,2'-(2,6-pyridine)-5,5'-bibenzimidazole (py-PBI) was used as the starting polymer for the preparation of the membranes, both pure and composites. Py-PBI was synthesized by means of microwave-assisted polycondensation between diaminobenzidine and 2,6-pyridinedicarboxilic acid (Sigma Aldrich assay >99%). The chosen fillers were mesoporous silica (SBA-15) and SBA-15 functionalized with different contents of propylsulphonic groups (10 mol%: SBA-SO$_3$H10, and 50 mol%: SBA-SO$_3$H50). In particular, four types of materials were used as separators for the MFC assembly: pure py-PBI, py-PBI/SBA-15, py-PBI/SBA-SO$_3$H10 and py-PBI /SBA-SO$_3$H50. The filler amount was 30 wt% with respect to the polymer. The SBA-15 based fillers were synthesized by sol-gel template route, as reported elsewhere [15, 16].

All the membranes were prepared by spraying method, as reported in a recent paper [17]. In particular, 16 cm^2 films of py-PBI and composites were obtained by spraying a proper volume of the polymer starting solution (PBI in DMSO 3wt%) with a spray gun on a plate heated at 150 °C. In case of composite systems, the filler was first dispersed in the starting solution, which was subsequently sonicated for about 30 minutes. The resulting membranes had thickness of about about 40 μm.

2.1.b Preparation of the Nafion^{TM}-based membrane

Nafion^{TM} 117 (20 wt% in ethanol) was used as the starting polymer for the preparation of the membranes In particular, 16 cm^2 film of Nafion^{TM} was obtained by spraying a proper volume of the polymer starting solution with a spray gun on a plate heated at 70 °C. The resulting membrane (thickness ~60 μm) was then activated by the following subsequent steps: i) immersion in a boiling H$_2$O$_2$ solution (3 wt%) for 1 h, ii) washing in distilled water, iii) immersion in a boiling solution of H$_2$SO$_4$ 0.5 M for 1 h, and finally washing three times in distilled water for 15 min.

2.1.c Preparation of the electrodes and cell configuration

Single-chamber MFCs (scheme 1) were assembled by using Py-PBI and Py-PBI-based composites as PEMs, Pt-C (40%) on carbon cloth as the air cathode and pure carbon paper as the anode.
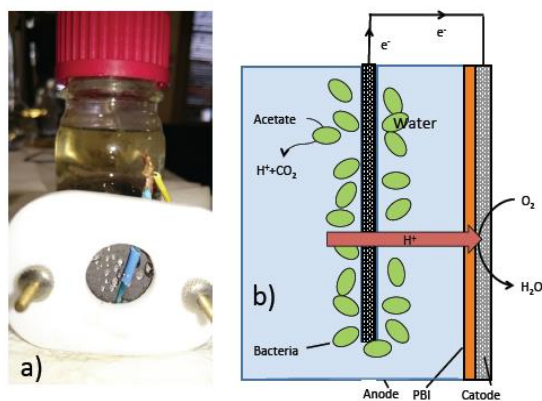
Scheme 1: PBI-based single-chamber MFC

In particular, the open-to-air cathode was fabricated by spraying a dispersion of platinum and carbon black onto a gas diffusion layer (SGL carbon – Sigracet 34bc) in order to have a Pt loading of 0.5 mg cm^{-2}. The ink was composed by 22.5 mg of Pt/C in 9 mL of DMA, added to 0.15 ml of the starting ionomer solution (Py-PBI in DMA, 3%$_{w/w}$). The anode was plain SGL carbon paper. The membrane and the cathode layers (catalyst side) were assembled by hot pressing at 130 °C under 1 ton for 10 minutes. The anode-projected area was 56 cm^2 (both sides of the electrode) whereas the cathode-projected surface was 8 cm^2 in case of MFCs based on Nafion^{TM}, and 4 cm^2 for the cells mounting composites with sulphonated SBA-15 silica.

The anode and the membrane/cathode assembly were placed in a 100 mL glass bottle with a working volume of 75 mL, with the anode placed at about 1 cm from the membrane.

All MFC reactors were operated at room temperature in a fed-batch mode, after inoculation performed by using returned sludge taken from an activated sludge process (Milan Domestic Wastewater Treatment Plant, Italy). The experiments were carried out in duplicate to check the system reproducibility. To have a better control on the original real waste-water and to avoid the growth of undesired microorganisms during the long-term experiments, the electro-active bacteria were fed with a 10 mM solution of CH_3COONa each week as the carbon source (namely 200 mg/week in the anodic chamber), whose COD was 2700 mg L^{-1}. A buffered nutrient solution (pH=7) consisting of KH_2PO_4 (5.8 g L^{-1}), K_2HPO_4, (10.0 g L^{-1}), NH_4Cl (0.1 g L^{-1}) and $MgSO_4.7H_2O$ (0.01 g L^{-1}) was also added.

The cells were kept under an external load of 100 ohm before the measurements, which were always carried out at pH=7. The conductivity of the solution was ~10^{-2} mS cm^{-1}.

2.2 Measurements

The surface morphology of the membranes before and after the experiments was observed by using a scanning electron microscope (Zeiss MA10). The samples were previously gold-sputtered. The images were collected by deeply mapping the sample at different magnitudes.

The membrane proton conductivity was measured by means of impedance spectroscopy, connecting a frequency response analyser (FRA Solartron 1255) to an electrochemical interface (Solartron 1287). The membrane was fixed to a four-points BekkTech conductivity cell, connected to the test stand BekkTech 411 for the temperature control. The impedance scans were performed at 30 °C and at 100% R.H. The impedance spectra were fitted with the ZView 3.0 software (Scribner Associates, Inc.).

The electrochemical tests were performed throughout the whole experimental period (2000 hours). In particular, the overall polarization curves were collected at room temperature by means of an electrochemical interface (Solartron 1287) scanning the potential from Open Circuit Voltage (OCV) to 0 V, at 0.1 mV s^{-1}. The impedance spectra of the cells were collected over the frequency range 0.1 Hz -100 kHz at voltage amplitude of 100 mV. The values of total resistance, R_i, were obtained by circular or linear best-fits (ZView 3-0, Scribner). No equivalent circuit models were used.

COD measurements were carried out by means of HACH COD analyzer, using a ISO-15705 Kit. The contact angles were obtained with a CAM200 (KSV) apparatus, using 5 microliters of water and averaging over five measurements.

The coulombic efficiency, ε_{cb}, was calculated over a period of time t_b by taking into account that in a MFC working in fed-batch mode, as in the present case, ε_{cb} is defined by the following equation:

$$\epsilon_{Cb} = \frac{M \int_0^{t_b} I \, dt}{F b v_{An} \Delta COD}$$

where M is the molar mass of oxygen, F is the Faraday's constant, b is the number of electrons exchanged during the electrochemical reaction per mole of O_2, V_{an} is the volume of the liquid in the anode compartment (75 mL), and Δ_{COD} is the COD change over the time of the experiment.

2. Results and Discussion

3.1 The PBI-based composite membranes

The use of inorganic fillers is a promising strategy to improve some properties of the PBI-based PEMFCs [12]. Recently, we prepared several PBI composite membranes for chemical fuel cells by dispersing SBA-15 and sulphonated SBA-15 in Py-PBI, so obtaining systems with improved mechanical properties, optimized acid doping level and, in the case of as prepared SBA-15, enhanced proton conductivity [15, 16]. Three composites were prepared starting from Py-PBI and a mesoporous silica, SBA-15, pristine and functionalized by two different molar amounts of sulphonic groups (10 mol% and 50 mol%, named SBA-SO$_3$H10 and SBA-SO$_3$H50, respectively). All these materials were here tested as PEMs for single-chamber MFCs, to investigate the influence of the filler on the functional properties of the separator. These devices were compared to a cell with a Nafion117^{TM} membrane as the separator.

Silica-based hybrid fillers differ for both microstructure and morphology depending on the functionalization degree. In our recent study [15], by means of solid state NMR, TEM and XRD we stated that the SO$_3$H$^-$ units have different spatial distribution along the silica backbone depending on their concentration. In the case of SBA-SO$_3$H10, the filler retains the ordered mesostructure of SBA-15 and the sulphonic groups are arranged both inside and around the nanosized channels of the network. In contrast, SBA-SO$_3$H50 shows small mesoporous domains inside a disordered silica structure. Here, SO$_3$H moieties are only partially arranged into the nanochannels [16].

Dispersions of filler up to 30 wt% into PBI were obtained by means of a spray technique recently developed in our laboratory [17]. By this way, we obtained highly homogeneous membranes with good free-standing properties, contrary to what occurs for Nafion^{TM}, where the maximum amount of silica compatible with good film mechanical properties did not exceed 5 wt%. Thanks to the good mechanical properties, we could fabricate relatively thin (~40 μm) membranes, which helped to reduce the contribution of the separator to the overall cell ohmic resistance. The proton conductivity of Py-PBI and Py-PBI-based composites was measured at 30 °C and 100% relative humidity, RH, after boiling in water for 2 hours. A value of 0.0016 mS cm^{-1} was obtained in case of pure Py-PBI, The conductivity remarkably increased in the composite systems, from 0.05 for Py-PBI/SBA-15 to 0.13 mS cm^{-1} and 0.5 mS cm^{-1} for Py-PBI/SBA-SO$_3$H10 and Py-PBI/SBA-SO$_3$H50, respectively.

The PBI-membranes resulted more hydrophilic than Nafion^{TM}. As proved by contact angle measurements, reported in table 1.

8

3.2   Long-term functional performances of single-chamber MFCs based on PBI membranes.

The bioelectrochemistry of open-to-air MFCs based on PBI PEMs was investigated by means of long-term operation experiments, carried out on all the devices over 100 days. The cells were kept under similar conditions in terms of substrate and fed-batch cycles and compared to Nafion117^{TM}, in order to address the actual role of both membrane and filler on the MFC functional stability and properties. Table 1 reports the properties of each studied system in terms of power density, normalized with respect to electrodes surface (PD_{an} and PD_{cat}) as well as bioreactor volume (PD_v), C.O.D. removal, coulombic efficiency and cell internal resistance. The electrochemical characterization was performed by means of polarization tests and impedance spectroscopy. The polarization curves were collected each week throughout a test period of 100 days, after that the microbial acclimation was complete. We defined the acclimation complete when the cell open circuit voltage, OCV, did not change more than 5% during 24 hours. The plots were obtained by linear voltammetry, by scanning the potential between OCV and 0 V at low scan rate (0.1 mV s^{-1}) in order to avoid power overestimation [7]. Figures 1 and 2 compare the voltage and power density (PD) curves vs. current density obtained after 100 operation days for the investigated MFCs.
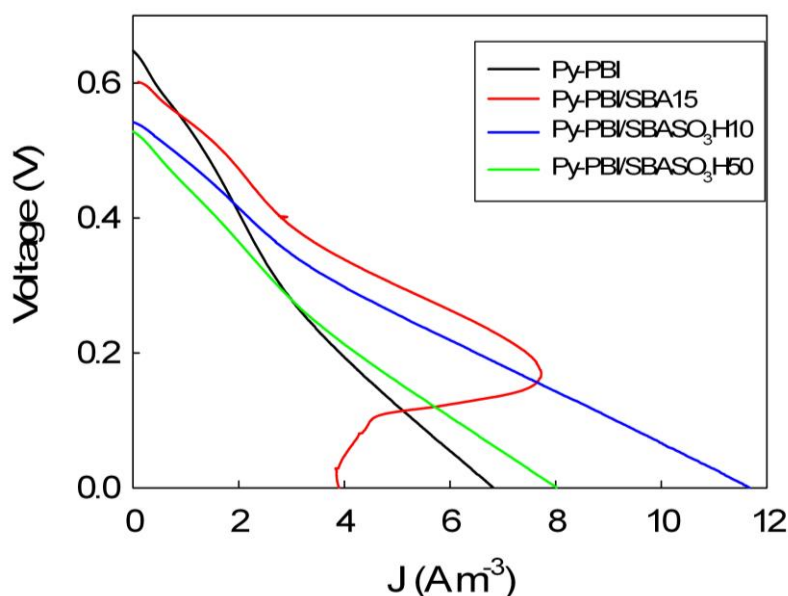

Fig. 1 Polarization plots, after 100 days of operation, of the investigated MFCs based on different PBI PEMs: unfilled Py-PBI (black line); Py-PBI/SBA-15 (red line); Py-PBI/SBA-SO$_3$H10 (blu line); Py-PBI/SBA-SO$_3$H50 (green line).
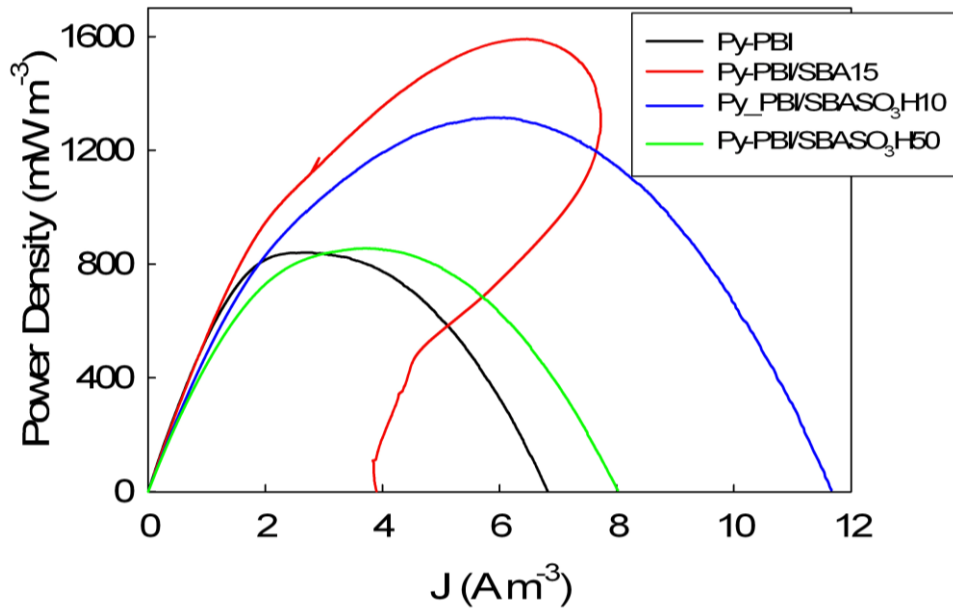
Fig. 2 Power density (normalized to the bioreactor volume) vs. current density after 100 days of operation of the investigated MFCs based on different PBI PEMs: unfilled py-PBI (black line); Py-PBI/SBA-15 (red line); Py-PBI/SBA-SO$_3$H10 (blu line); Py-PBI/SBA-SO$_3$H50 (green line).

Table 1 reveals good MFCs performances when the separator is a composite membrane of py-PBI. Indeed, the maximum PD generated by the PBI cells is remarkably higher than that provided by Nafion^{TM}-based devices, in some case even more than by one order of magnitude. The best power output was obtained with the composite separator with silica containing 10 mol% of sulphonic groups, Py-PBI/SBA-SO$_3$H10, which showed a peak of power density, PD_v, exceeding 1300 mW m^{-3} ($PD_{cat}>160\ mW\ m^{-2}$) after 100 working days.

Membrane	PD_v (mW m^{-3})	PD_{an} (mW m^{-2})	PD_{cat} (mW m^{-2})	OCV (V)	R_s (Ω)	R_f (Ω)	ε_c (%)	COD r.r. (mg dm^{-3} h^{-1})	Contact angle (°)
Py-PBI	844	11.4	78.3	0.66	443	671	20	13.0	55±5
Py-PBI/SBA15	1521	21.3	148	0.60	154	164	14	14.3	59±2
Py-PBI/SBA15-SO$_3$H10	1312	17.6	169	0.54	164	275	31	7.3	60±10
Py-PBI/SBA15-SO$_3$H50	852	11.3	260	0.53	545	414	28	7.8	58±7
Nafion^{TM}	129	1.7	12	0.36	212	3936	22	5.1	96±5

Table 1: Physico-chemical and functional properties of MFCs based on PBI membranes, working at room temperature with a load of 100Ω, after 96 days of batch feeding. PD_v: maximum volumetric power density delivered by the cell; PD_{an}: Maximum Power Density to anode; PD_{cat}: Maximum Power Density to cathode; R_s and R_f: total cell resistance at the beginning and at the end of experiment; ε_c: coulombic efficiency; COD r.r.: COD removal rate; contact angle. The properties of Nafion117^{TM} are reported for the sake of comparison.

The cell based on PBI filled by pure SBA-15 provided also a higher PD maximum ($PD > 1500\ mW\ m^{-3}$, $PD_{cat}=148\ mW\ m^{-2}$). However, in this case, an important overshoot occurs, as clearly shown by Figures 1 and 2. Here the power density plot doubles back to lower current after that the

maximum PD is achieved. This kind of overshoot is frequently reported in the literature [7], and may be interpreted as a result of an immature biofilm, which is not able to adapt itself to high currents demand [18]. In contrast, the other PBI cells do not show evidence of curve distortion and this is the indication of a quite stable biofilm formed at the anode compartment during the anode-enrichment period and the fed-batch cycles.

In order to evaluate the role of the membrane on the MFC durability, long-term experiments were carried out. Figure 3 shows the maximum power density, PD_{MAX}, vs. the device operating time.
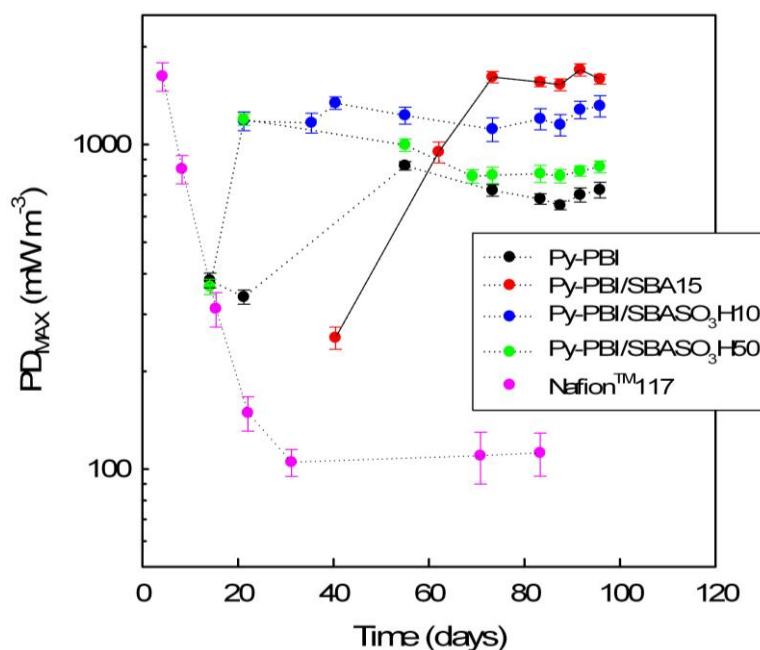

Fig. 3 Time-dependent behavior of the Maximum Power Density for MFCs based on different PEMs: unfilled Py-PBI (black); Py-PBI/SBA-15 (red); Py-PBI/SBA-SO$_3$H10 (blue); Py-PBI/SBA-SO$_3$H50 (green); Nafion117^{TM} (pink).

In case of unfilled Py-PBI, the maximum power density was achieved after about 50 days ($PD_v=840\ mW\ m^{-3}$, $PD_{cat}=78.3\ mW\ m^{-2}$), whereas longer times were required for Py-PBI/SBA-15, which reached the top after about 70 days of operation ($1600\ mW\ m^{-3}$). In contrast, the cells based on the composite membranes with sulphonated silica, Py-PBI/SBA-SO$_3$H10 and Py-PBI/SBA-SO$_3$H50, showed their maximum performances ($PD_v=1300\ mW\ m^{-3}$, $PD_{cat}=169\ mW\ m^{-2}$, and $PD_v=850\ W\ m^{-3}$, $PD_{cat}=260\ mW\ m^{-2}$, respectively) in a much shorter time, namely twenty days. Generally speaking, the power density behavior is quite stable. Py-PBI and the composite with SBA-SO$_3$H50 showed limited decreases during the whole operation period after the maximum PD was achieved (29% and 18%, respectively). Better performances were provided by the cell with Py-PBI/SBA-SO$_3$H10, whose power output remained nicely constant during the entire 100 days

of operation. Contrary to what observed for PBI-based MFCs, our reference Nafion^{TM} cell reaches its maximum power density in only 4 days (1600 mW m^{-3}), but the electrochemical performances rapidly fell down by more than a factor of ten after 20 days, reaching a plateau at 100 mW m^{-3} ($PD_{cat}=12\ mW\ m^{-2}$).

The long-term durability of the PBI-based MFCs is a very promising result. In fact, significant power drops with time were frequently reported in literature [18], which were attributed to a number of biological, electrochemical and physico-chemical factors, including non-optimal external load, precipitation of salts at the cathode, biofilm thickness increase, nutrients diffusion and membrane biofouling.

In the present case, the differences in functional properties observed among the membranes, and mostly between the PBI and Nafion^{TM} systems (about one order of magnitude in power density), may be interpreted by taking into accounts several aspects, first the membrane biofouling (as it will be discussed in details in the following section), but also other factors related to the system microstructure. It is well known from the literature that the performances of Nafion^{TM} and Nafion^{TM}-like PEMs depend on the number of side-chain–SO$_3$H groups, which are responsible for the proton transport. Such moieties could be negatively affected by the coordination of the H-binding sites to cations present in the substrate, at the expense of protons, so enhancing the membrane resistance to proton transport [11]. In contrast, the PBI systems do not show such a problem. The performances of Py-PBI MFCs are improved by dispersing SBA-15 silica filler into the membrane. The addition of silica functionalized with sulphonic groups also has beneficial effects, which, however, are dependent on the SO$_3$H amount and on the microstructural properties of the SBA-based particles [15, 16]. Here, the membrane Py-PBI/SBA-SO$_3$H10 gives the best performances. This is likely due to the fact that in SBA-SO$_3$H10 filler a significant fraction of the sulphonic units are placed inside the silica mesopores, so resulting less available to be coordinated by the metal ions of the substrate. The actual proton transport in case of SBA-SO$_3$H10 composite is improved with respect to the other membranes, because protons have additional pathways (given by SO$_3$H groups inside the pores) for migration.

In case of Py-PBI/SBASO$_3$H50, the filler meso-structure is partially destroyed, therefore most acidic units are distributed along the surface, which is now available for the coordination of the bigger cations (e.g. Na$^+$, K$^+$, Ca^{2+} etc.) coming from the substrate. The resulting performances are less stable than those of Py-PBI/SBA-SO$_3$H10 but still better than those of the unfilled Py-PBI (see Table 1 and Figure 3).

Membrane biofouling is one of the most critical issues responsible for the deterioration of the electrochemical MFCs performances on long-term operations. The negative effect of PEM fouling was demonstrated in the literature by comparing fresh, fouled and cleaned cells. Net improvements of power output and functional stability after periodical physical and chemical cleaning steps were reported [7, 11, 18].

Here, biofouling of cells was investigated by SEM, and remarkably different behaviours were observed depending on the nature of the composite membrane. Figure 4 reports the SEM images of the membranes (anode site) after 100 days of MFC operation. There is a substantial difference between the large biofouling of Nafion^{TM} and that very small of Py-PBI.
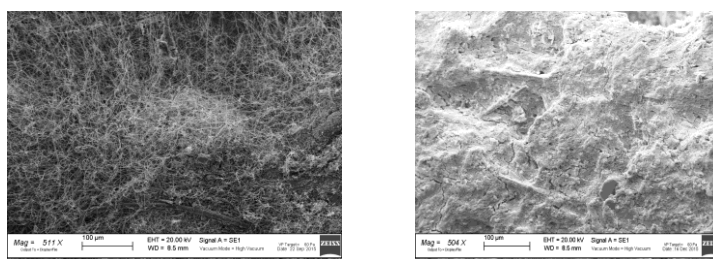

Fig. 4 Comparison of SEM images of a Nafion^{TM} membrane (left) and a Py-PBI membrane (right), after 100 days of operation.

The SEM images of Figure 5 shows very small biofouling levels in all py-PBI membranes. Only some microorganisms can be observed on py-PBI and Py-PBI/SBA-SO$_3$H50. In particular, the microbic population seems to be round-shaped (~10 μm), growing onto a layer of fair sized rod-shaped coccoids (~1 μm), which stick on the membrane surface and form long chains. In contrast, SEM images of the Py-PBI/SBA-15 and Py-PBI/SBA-SO$_3$H10 membranes reveal only the presence of inorganic salts precipitated from the substrate and the absence of a bulky biolayer.
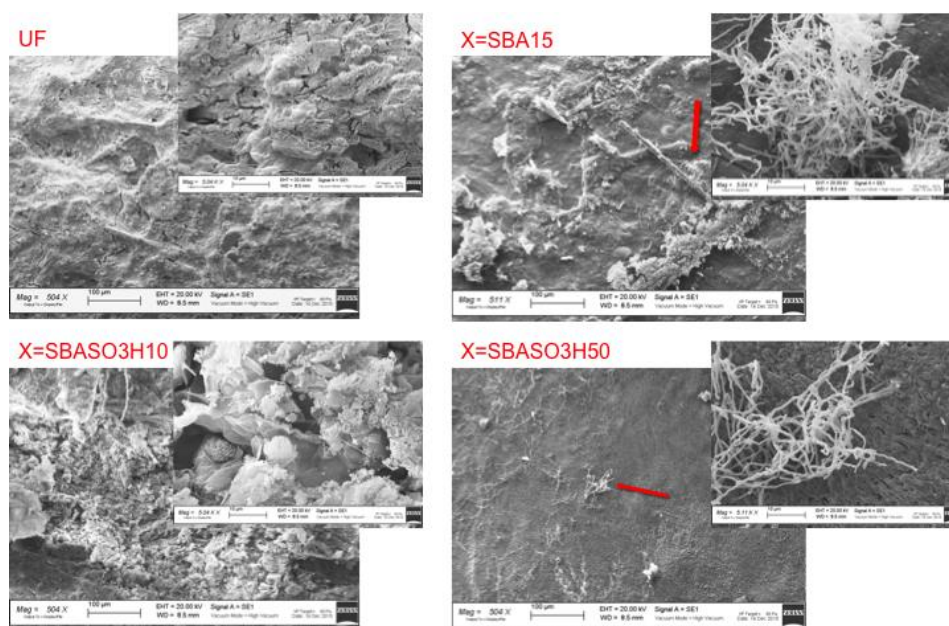
Fig. 5 SEM images of Py-PBI, unfilled and composite membrane surface after 100 days of operation.

The biofouling extent of the membranes is in agreement with the power results obtained by the polarization process. In particular, the absence of biofouling in Py-PBI membranes, both unfilled and composite, could justify the much better MFC results. In the absence of specific biochemical/microbiological analyses, we are not able to explain why PBI is so resistant to biofouling, but some hypotheses could be formulated by taking into account what already discussed in literature [see for instance ref. 10.]

The different amount of biofouling between Py-PBI and Nafion^{TM} could be likely explained by the different permeability to oxygen. While Nafion^{TM} is known to be highly permeable to oxygen (10^{-11} – 10^{-12} mol/(cm s bar)), PBI permeability is 5×10^{-15} mol/(cm s bar) at room temperature [19]. Indeed, the micro-environment near a permeable membrane could favour the growth of aerobic bacteria colonies and promote the formation of a biofilm [10].

Electrochemical impedance spectroscopy (EIS) is used to estimate the MFC internal resistance, R_i, in order to determine the contributions of each cell component in case of non-linear polarization plots. In the present study, the data were collected every week during the whole operation period. Figure 6 reports the spectra obtained once the cell acclimation was achieved, and at the end of the long-term experiment.

In case of air-cathode MFCs, the total resistance, R_i, is representative of several contributions [21], namely the activation and the diffusion resistances related to the polarization at both bio-anode ($R_{a,a}$, $R_{a,d}$) and bio-cathode ($R_{c,a}$, $R_{c,d}$), the ohmic resistance (R_Ω) and the middle

components resistances, e.g. the ion-exchange membrane one (R_m), as described by the following equation [20]:

$$R_i = R_\Omega + R_m + R_{a,a} + R_{a,d} + R_{c,a} + R_{c,d}$$

The Nyquist plots obtained after the acclimation on the MFCs based on the PBI composite membranes only show the intercept on the Z real axis at high frequency, contrary to the unfilled system which shows also an additional resistive contribution at lower frequency.
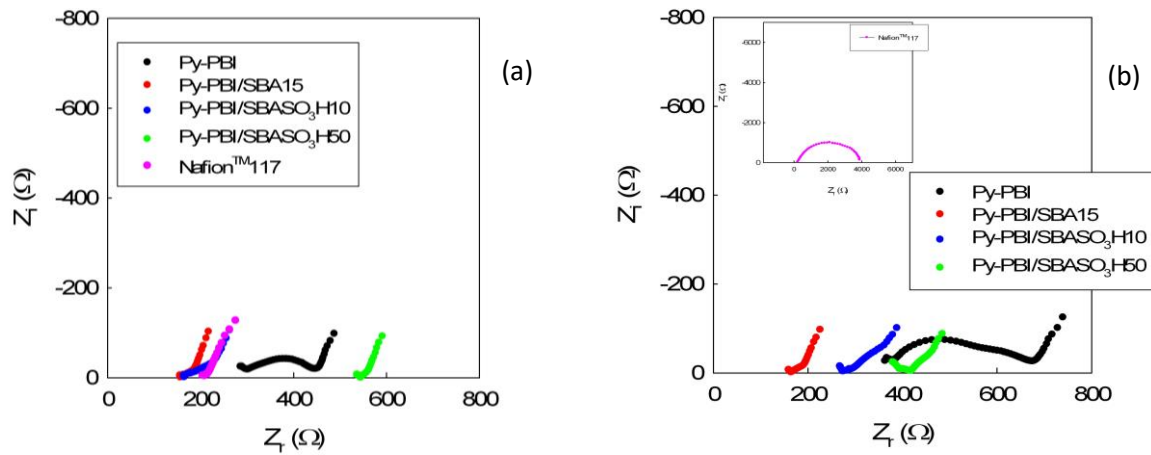

Fig. 6 Impedance spectra of MFCs based on different PEMs after that cell acclimation was achieved (a), and after 100 days of operation (b). Unfilled Py-PBI (black); Py-PBI/SBA-15 (red); Py-PBI/SBA-SO$_3$H10 (blue); Py-PBI/SBA-SO$_3$H50 (green); Nafion^{TM} (pink). In panel (b) the curve of Nafion^{TM} is reported in the inset.

Since the best-fitting of the data in terms of equivalent circuit models is not easy because of the scarce spectra structure, we will limit ourselves to phenomenological considerations based on recent literature [20]. The values of total resistance at the beginning and the end of operation, R_s and R_f respectively, as determined by simple spectral analysis (see Experimental Section), are listed in Table 1 for each sample. At the end of the long-term experiments (about 100 days), the resistance values increase of 10-40% depending of the membranes, except for Py-PBI/SBA-SO$_3$H50 where a slight decrease was observed. For what concerns Nafion^{TM}, a resistance value exceeding 3700 Ω was measured at the end of the long-term experiment. Such a difference may be again interpreted in terms of the thicker biofouling layer deposited on the Nafion^{TM} surface compared to the PBI-based membranes, as shown by SEM images reported in Figures 4 and 5.

3.4 Wastewater treatment efficiency

The MFCs efficiency in the treatment of the domestic wastewater was investigated by measuring the chemical oxygen demand (COD) during the operation time and the coulombic efficiency, ε_c, defined as the ratio between the total charge actually transferred to the anode from the substrate, and the maximum possible charge obtained if all the substrate removal should produce electric current

Figure 7 reports the COD removal during the first 140 hours of experiment, calculated as the ratio between the removed and influent COD values. This parameter determines the amount of fuel converted into bioelectricity by MFC, and is required to calculate the actual electrochemical efficiency of the purification treatment, expressed in terms of the coulombic efficiency, ε_c.
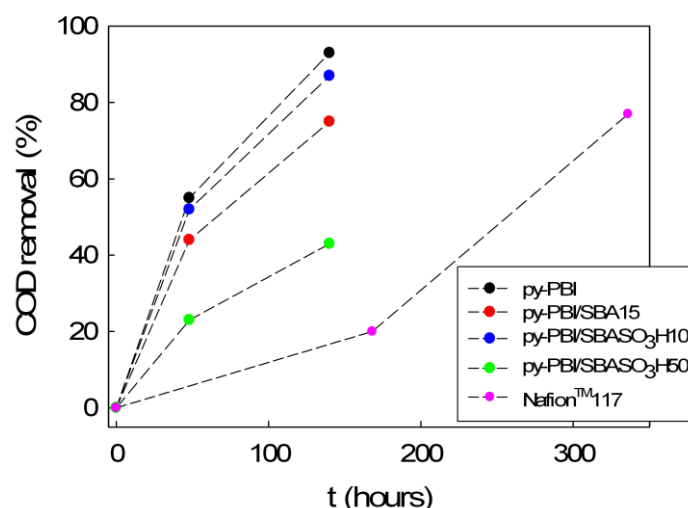

Fig. 7 COD removal efficiency for the investigated MFCs with time. Unfilled Py-PBI (black); Py-PBI/SBA-15 (red); Py-PBI/SBA-SO$_3$H10 (blue); Py-PBI/SBA-SO$_3$H50 (green). Nafion^{TM} COD (pink) is also reported for the sake of comparison.

The best performances were offered by unfilled Py-PBI and the composite Py-PBI/SBASO$_3$H10, which achieved COD removal exceeding 90% after 140 hours of operation. Lower removal capacity was observed in case of the other PBI composites, and particularly by Py-PBI/SBASO$_3$H50. A very interesting result emerges by comparing the COD removal rates observed for the PBI- and Nafion^{TM}-based cells. The PBI-based cells are much more efficient than Nafion^{TM}. In fact, after 140 hours Nafion^{TM}-MFC removed only 20% of the initial chemical oxygen demand, contrary to 93% determined for Py-PBI.

As already stated, the COD is used to determine the MFC coulombic efficiency, ε_c [21]. Table 1 reports the coulombic efficiency of the PBI-based MFCs, which ranges between 14% in the case of unfilled Py-PBI/SBA-15, and 31% for Py-PBI/SBA-SO$_3$H10 after 140 hours of operation. The value obtained for the MFC with Nafion^{TM} after 336 hours of operation is also reported for the sake of comparison. Again, the cell with the composite Py-PBI/SBA-SO$_3$H10 resulted very promising. In fact, the MFCs coulombic efficiency reported in literature for the treatment of domestic wastewaters typically is less or equal 20% during the first 2-3 weeks of working time [7]. This result is a further demonstration of the positive effect of our sulphonated filler (SBA-SO$_3$H10) on the performances of the PBI-composite membrane as a separator for MFCs.

3.5   Sustainability of PBI-based MFCs: Environmental and cost assessment.

Table 2 reports the cost comparison between Polybenzimidazole and other systems, tipically used as membranes for MFCs. PBI is a quite low-cost polymer. The cost-effective aspect is one of the key-factor, which has gathered the attention of both research and development in such systems for what concerns the application as membranes also in chemical fuel cells [22]. Its cost is estimated to be about 30 €/m^2, remarkably lower than that one reported for Nafion^{TM}- and Nafion^{TM}-like polymers, which ranges around 900 €/m^2, depending on the type of membrane. PBI is also cheaper than some cation exchange membranes, as for instance CMI-7000, whose price is around 150 €/m^2. Polybenzimidazole-based systems may be even a possible substitute of some ceramic membranes, as for instance mullite, the price of which is lower than 20 €/m^2, as shown in table 2. Table S2 (see supplementary materials) shows as an example the power density and the membrane price for some MFCs including PBI-, Nafion^{TM}- and commercial mullite as membrane electrolytes. Indeed, by comparing the price/power ratios, PBI-based MFCs seem to be particularly efficient for what concerns the power generation cost.

Membrane Material	Price (€ m^{-2})
PBI [a]	30
Nafion^{TM} [b]	900-1000
CMI-7000^{TM} (CEM) [c]	150
Mullite [d]	16
Earthenware [d]	5
Pyrophillite [d]	450
Alumina [d]	136

Table 2: Average cost of the materials used for the preparation of the MFC membranes. (a) data available from ref. 22; (b) data available from R.S.L. Yee et al., Chem. Eng. Res. Des. 90 (2012) 950; (c) from www.membranesinternational.com; (d) data available from ref. [18].

To gain an insight on the sustainability of the proposed devices, we carried out an environmental assessment based on the use of Green Metrics tools, [23-25] focusing on the materials employed to build the Py-PBI based membranes, and comparing the results with those of the Nafion^{TM} cell. In particular, we adopted the EATOS (Environmental Assessment Tool for Organic Syntheses) [24-26] software to model the cost (both environmental and economic) involved in the preparation of 1 kg of material of membranes containing either the PBI or the Nafion^{TM} polymers.

The EATOS method allows quantitative analysis for assessing the environmental burdens and human risks related to the use of chemicals, through the use of easily available data (mainly available in the Material Safety Data Sheets - MSDS) [26]. The analysis is based on five different indexes, considering respectively the quantity and quality of chemicals, as well as the economic cost. The first two indexes deal with mass, where the quantities of raw materials and resulting waste referred to the production of 1 kg of the desired substance are evaluated. These parameters are indicated, respectively, as S^{-1} (the selectivity index, equivalent to the PMI index) [27-32] and E (the E-Factor proposed by Sheldon) [33], and are expressed in kg·kg^{-1} units. Two further Environmental Indexes, named EI$_{IN}$ and EI$_{OUT}$, are available and can be calculated by multiplying, respectively, the terms contributing to S^{-1} and E by appropriate weighting factors, Qi. Both EI$_{IN}$ and EI$_{OUT}$ are expressed in terms of PEI·kg^{-1}, where PEI stands for "Potential

Environmental Impact". Indeed, the Qi values account for: i) the environmental and social costs involved in the production of the chemicals used, and ii) the damage to the surrounding ecosystem caused by the chemicals produced. Accordingly, the Qi values can be ≥ 1, the higher the Q value the more dangerous the chemical. Finally, the EATOS software also provides an Economic Index, indicating the actual cost related to the production of 1 kg of the desired chemical, expressed as $€\cdot kg^{-1}$.

Since the EATOS software is commonly adopted to assess syntheses, in the case of the PBI membrane we modeled the formal reaction between the polymer and silica (the substrates) to prepare the final membrane (the product), also taking into account the employed solvents. Indeed, all of the required input data (physico-chemical properties, price, risk and safety phrases, transport information, ecological parameters, acute and chronic toxicity, etc.) are available in the MSDS from the suppliers (see Supporting Information and Table S1 for more details).

The results obtained from the assessment procedure are reported in Figure 8. As for the mass indexes (see Fig. 8a), the environmental impact involved in the production of 1 kg of the PBI membrane is approx. twice as that of the Nafion^{TM} membrane. This is related to the different amount of solvents used in the two procedures, where in the former case a 1:1 water/ethanol mixture is used, while in the latter a double volume of DMSO (that has a higher density) is adopted. Turning to the environmental indexes gathered in Fig. 8b, a similar scenario is shown. However, it is interesting to consider separately the impact from substrates (contributing to the EI_{IN} index only) and solvents (contributing to both EI_{IN} and EI_{OUT} indexes). Indeed, in the production of both membranes, non-hazardous solvents are used, apart from flammable ethanol (resulting in a slightly higher Q_i value).
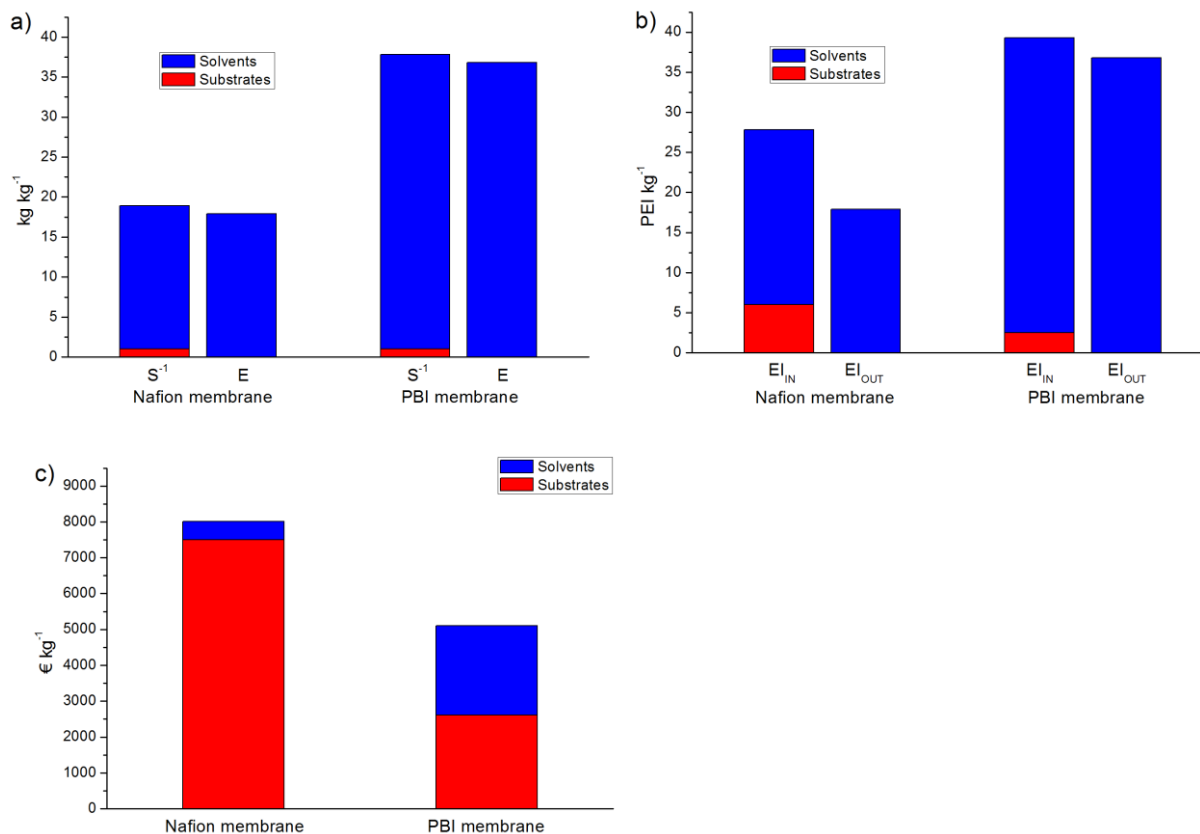
Fig. 8 EATOS assessment of the membranes studied in the present work: a) mass indexes; b) environmental indexes and c) economic index.

Accordingly, the preparation of the Nafion^{TM} membrane remains advantageous, due to the different amounts of employed solvents. The situation is different, however, in terms of employed substrates, since the PBI membrane shares a lower environmental impact with respect to the Nafion^{TM} one. This is due to the high cost of Nafion^{TM}, which increases the corresponding Q_i value and, therefore, the overall impact with respect with the PBI polymer. As for the economic index (see Fig. 8c), the PBI membrane results advantageous over the Nafion^{TM}-based one, again due to the contribution of Nafion^{TM}, that accounts for more than 90% of the overall cost. By contrast, a more balanced situation is observed in the PBI membrane, where the principal contributions are due to the employed silica and the solvent, while the polymer contributes only in minimal part (about 10%).

Indeed, our analysis is performed on a lab-scale device, and must be deepened in order to consider the steps towards the industrial level. We stress here EATOS should not be intended as a full Life Cycle Assessment. In particular, energy costs, manpower, capital costs, materials lifetime, solvent recyclability, ease of plant scaling, etc. should be properly considered in order to obtain a more realistic insight.

4. Conclusions

Four Py-PBI-based PEMs, the unfilled polymer and different composites, were tested as separators for open-to-air-cathode MFCs, operating in fed-batch mode for urban wastewater treatment. The composites were obtained by dispersing into the polymer 30 wt% of mesoporous silica (SBA-15) and of the same silica functionalized with sulphonic groups. The results were compared with those of a MFC including Nafion117^{TM} as the separator.

All the investigated cells with PBI as PEM showed better results with respect to Nafion^{TM}, in terms of power density, cell durability and treatment efficiency. The MFC based on Py-PBI/SBA-SO$_3$H10 membrane showed the best performances: i) a maximum power density exceeding 1.3 W m^{-3} without any power loss after 100 days, ii) good efficiency with a very high COD removal (more than 90%), and iii) high coulombic efficiency (31%) after only 6 days, which is an excellent result in case of natural wastewater.

Moreover, the use of PBI membranes preserved MFC from biofouling issues. Indeed, this polymer inhibits the microbial adhesion, contrary to what occurs for Nafion^{TM}, whose surface is covered by a dense bacterial colony, which dramatically affects the cell performances over long-term operation.

References

[1]. U. Schroeder, ChemSusChem 5 (2012) 959.

[2]. W.-W. Li, H.-Q. Yu, Z. He, Energy Environ. Sci. 7 (2014) 911.

[3]. P. Pandey, V.N. Shinde, R.L. Deopurkar, S.P. Kale, S.A. Patil, D. Pant, Applied Energy 168 (2016) 706.

[4]. U. Schroeder, F. Harnisch, L.T. Angenent, Energy Environ. Sci. 8 (2015) 513.

[5]. A. Rinaldi, B. Mecheri, V. Garavaglia, S. Licoccia, P. Di Nardo, E. Traversa, Energy Environ. Sci. 1 (2008) 417.

[6]. G.G. Kumar, V.G. Sathiya Sarathi, K.S. Nahm, Biosensors and Bioelectronics 43 (2013) 461.

[7]. B.E. Logan, ChemSusChem 5 (2012) 988.

[8]. M. Zhou, H.Wang, D.J. Hassett, T. Gu, J. Chem. Technol. Biotechnol. 88 (2013) 508.

[9]. S.M. Daud, B.H. Kim, M. Ghasemi, W.R.W: Daud, Biores. Tech. 195 (2015) 170.

[10]. J.X. Leong, W.R. Wan Daud, M. Ghasemi, K.B. Liew, M. Ismail, Ren. Sust. Energy Rev. 28 (2013) 575.

[11]. S. Sevda, X. Dominguez-Benetton, K. Vanbroekhoven, T.R Sreekrishnan, D. Pant, Chemical Engineering Journal 228 (2013) 1.

[12]. E. Quartarone, P. Mustarelli, Energy Environ. Sci. 5 (2012) 6436.

[13]. S. Singha, T. Jana, J. J.A. Modestra, A. Naresh Kumar, S.V. Mohan, J. Power Sources, 317 (2016) 143.

[14]. V. Kumar, S. Mondal, A. Nandy, P.P. Kundu, Biochem. Eng. J. 111 (2016) 34.

[15]. A.S. Cattaneo, D.C. Villa, S. Angioni, C. Ferrara, E. Quartarone, P. Mustarelli, J. Phys. Chem. C. 119 (2015) 18935.

[16]. A.S. Cattaneo, C. Ferrara, D.C. Villa, S. Angioni, C. Milanese, D. Capsoni, S. Grandi, P. Mustarelli, V. Allodi, G. Mariotto, S. Brutti, E. Quartarone, Micro. Meso. Mat. 219 (2016) 219.

[17]. E. Quartarone, D.C. Villa, S. Angioni, P. Mustarelli, Chem. Comm. 51 (2015) 1983.

[18]. G. Pasternak, J. Greenman, I. Ieropoulos, ChemSusChem, 9 (2016) 88.

[19]. H. Pu, Polymer for PEM fuel cells, Wiley, Hoboken, 2014, p. 267

[20]. X. Dominiguez-Benetton, S. Sevda, K. Vanbroekhoven, D. Pant, Chem. Soc. Rev., 41(2012) 7228.

[21]. B.E. Logan, B. Hamelers, R. Rozendal, U. Schroeder, et al., Environ. Sci. Technol. 40 (2006) 5181.

[22]. Q.Li, D.Aili, H.A. Hjuler, J.O. Jensen (Eds.). High temperature polymer electrolyte membrane fuel cells: Approaches, Status, Perspectives. Springer, Switzerland (2016).

[23]. S. Protti, A. Albini, Paradigms in Green Chemistry and Technology, Briefs in Green Chemistry for Sustainability, Springer, 2016.

[24]. F. G. Calvo-Flores, ChemSusChem 2 (2009) 905.

[25]. M. Eissen, J. O. Metzger, Chem. Eur. J. 8 (2002) 3581.

[26]. The EATOS software is available as a free download at: http://www.chemie.unioldenburg.de/oc/metzger/eatos/.

[27]. M. Pini, R. Rosa, P. Neri, F. Bondioli, A. M. Ferrari, Green Chem. 17 (2015) 518.

[28]. S. Toniolo, F. Aricò, P. Tundo, ACS Sustainable Chem. Eng. 2 (2014) 1056.

[29]. D. Ravelli, S. Protti, M. Fagnoni, A. Albini, Curr. Org. Chem. 17 (2013) 2366.

[30]. D. Ravelli, S. Protti, P. Neri, M. Fagnoni, A. Albini, Green Chem. 13 (2011) 1876.

[31]. S. Protti, D. Dondi, M. Fagnoni, A. Albini, Green Chem. 11 (2009) 239.

[32]. C. Jimenez-Gonzalez, C. S. Ponder, Q. B. Broxterman, J. B. Manley, Org. Process Res. Dev. 15 (2011) 912.

[33]. R. A. Sheldon, Green Chem. 9 (2007) 1273.